

## Paper

Int'l J. of Aeronautical & Space Sci. 17(1), 109–119 (2016)  
DOI: <http://dx.doi.org/10.5139/IJASS.2016.17.1.109>

# Part tolerancing through multical defect analysis

**Mathieu Petitcuenot\***

*LURPA, ENS Cachan, Univ Paris Sud, Université Paris-Saclay, 61 avenue du président Wilson, Cachan 94235, France  
Snecma, groupe SAFRAN, site de Villaroche, Rond-point René Ravaud – Réau, Moissy-Cramayel 77550, France*

**Bernard Anselmetti\*\***

*LURPA, ENS Cachan, Univ Paris Sud, Université Paris-Saclay, 61 avenue du président Wilson, Cachan 94235, France  
Université Paris-Sud, IUT de Cachan, 9, Avenue de la Division Leclerc, Cachan 94230, France*

## Abstract

When manufactured parts undergo large deformations during the manufacturing process, the global specifications of a part based on the concept of tolerance zone defined in the ISO 1101 standard [1] enable one to control the part's global defects. However, the extent of this tolerance zone is too large when the objective is to minimize local defects, such as hollows and bumps. Therefore, it is necessary to address local defects and global defects separately. This paper refers to the ISO 10579 standard [2] for flexible parts, which enables us to define a stressed state in order to measure the part by straightening it to simulate its position in the mechanism. The originality of this approach is that the straightening operation is performed numerically by calculating the displacement of a cloud of points. The results lead to a quantification of the global defects through various simple models and enable us to extract local defects. The outcome is an acceptable tolerance solution. The procedure is first developed for the simple example of a steel bar with a rectangular cross section, then applied to an industrial case involving a complex 3D surface of a turbine blade. The specification is described through ISO standards both in the free state and in the straightened state.

**Key words:** Tolerancing, Defect analysis, Digital straightening, Complex surface

## 1. The context and the scientific objective

### 1.1 The context

The problem addressed in this study is how to separate local defects (hollows, bumps, flat spots, jumps...) from global defects in parts which are supposedly rigid, but actually are distorted (Fig. 1).

In the first application, the part being considered has a constant cross section and is twisted or distorted due to the manufacturing process or to transportation. The part is straightened during assembly. Significant global defects are tolerated, but some residual defects can be unacceptable because of functional requirements, such as appearance.

The second example concerns the manufacturing of slender parts in which local defects must be detected because they could compromise strength or performance.

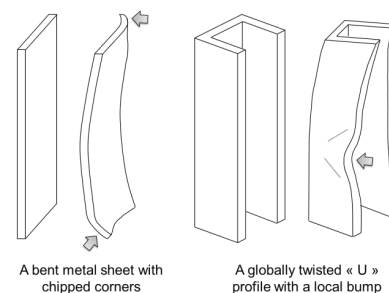


Fig. 1. Examples of parts and defects

This is an Open Access article distributed under the terms of the Creative Commons Attribution Non-Commercial License (<http://creativecommons.org/licenses/by-nc/3.0/>) which permits unrestricted non-commercial use, distribution, and reproduction in any medium, provided the original work is properly cited.



\* Ph. D Student, Corresponding author: [Mathieu.petitcuenot@lurpa.ens-cachan.fr](mailto:Mathieu.petitcuenot@lurpa.ens-cachan.fr)  
\*\* Professor

The detection of local defects requires the surface to be measured using a large number of closely-spaced points. The resolution must be adjusted to the size of the defect being sought. For example, using scanning or optical measurement techniques, the resolution can be as small as 0.3 mm. However, the objective is not to measure the roughness or waviness of the part.

Traditional form specification is unsuitable because acceptable global defects can be much larger than the maximum acceptable local defects.

Metrology techniques are used to compare the measured part to the nominal CAD model and display the deviations at various points. The specification is satisfied if all the points are inside the tolerance zone defined by the ISO 1101 standard [1].

In our new approach, an intermediate, distorted model (e.g. through twisting or bending) is defined. The residual deviation between the distorted model and the measured part is calculated. In addition, the parameters of the deformation can be used to assess the quality of the actual part.

## 1.2 Bibliographical review

This work discusses two applications in the fields of metrology, defect analysis, calculation and tolerancing. The measurements were carried out using a coordinate measuring machine for the first application and an optical measuring device for the turbine blade.

All measuring devices have their own characteristics and particularities. Li [3] presented a general state-of-the-art of various types of measuring machines. Even though the emphasis is primarily on CMM measurement, the characteristics, advantages and drawbacks of contact-free techniques for free-form inspection are also discussed.

Similarly, Savio [4] presented and compared contact and non-contact inspection tools along with some applications. His study focuses more particularly on the shape of a turbine blade and the problem of the distribution of points along the aerodynamic profile. The difficulty is that the curvature of an airfoil becomes very high near the thin edges. The choice of the density of the points on an airfoil is a common concern. In our work, the points were sampled on the pressure side and the suction side, excluding the edges in order to avoid problems in fitting the actual profile to the CAD model.

Several studies were aimed at the identification of manufacturing defects in parts.

Radvar-Esfahlan [5, 6] proposed an inspection methodology based on a knowledge of predictable defects, such as the effect of gravity or residual strains on large slender

parts. Assuming conservation of distance, he applied a finite element simulation to a CAD model, then performed rigid registration with the sampled scanned workpiece, and finally used non-rigid registration to eliminate the springback effect of the manufacturing process.

The registration of point clouds with the CAD model is an important step in the analysis process. Many works have used Bourdet's concept of small displacement torsor [7], which lends itself particularly well to small strains and small displacements. The next references used that approach to build mathematical models of defects.

Zhu [8] conducted an exhaustive study on the efficient registration of free-form surfaces. Along with Savio [4], he raised the issue of the point density of the sample. He used the root-mean-square error criterion, which depends on the entire sample of points rather than on the end points or boundary points alone. The least-squares method we used in this paper for registration and calculation led us to choose a homogeneous point distribution. Zhu noted that after he performed the registration the turbine blade became "slightly twisted": our work shows how such a defect can be identified and quantified.

Various types of models for the representation of parts with defects can be found in the literature along with the association method used to fit the model to the measured element.

The modal method developed by Samper [9] uses the identification of real surfaces from a defect base composed of a series of eigenmodes of the surfaces. The first eigenmodes are associated with a surface's size and position, then with its orientation. The subsequent modes present ripples of decreasing periods which can be used to represent sheer, concavity and all the smaller ripples which can occur on a surface. A Fourier model is used for the decomposition. This work can be extended to roughness.

In [10], Adragna presented a state-of-the-art review of the modal method, beginning with the techniques based on vibration studies, such as Formosa's work [11]. In addition, Adragna introduced shape defects called "technological modes". He proposed to create a modal basis composed of defects which may occur during the manufacturing process, but cannot be defined directly by decomposition into vibration modes. One of the drawbacks of the decomposition into eigenmodes is that the mode shapes are continuous, whereas a technological mode can include a peak, a step or an abrupt change of slope in the geometry. Adragna recommended that technological modes be put at the beginning of the modal basis because they are likely to occur frequently.

A similar approach was followed by Favrelières [12], who

characterized the actual geometry using a decomposition into an orthogonal basis of vibration modes.

Other methods of the same type have been developed, e.g., in the case of plane parts, the decomposition of shape defects into Fourier series by Capello [13] and the identification of shape defects by discrete cosine transform by Huang [14].

The analysis of shape defects in cylindrical surfaces was addressed in several works. For example, Summerhays [15] and Henke [16] recreated shape errors using an association of Fourier series and Chebyshev polynomials completed by a basis made of measured eigenmodes. Cho [17] carried out a similar study and compared his results with those of Damir [18].

These types of analyzes are applicable when the shape or the cause of the defect is unknown. Otherwise, the origin of the deviations can help define a mathematical model to represent the defect.

In the aviation industry, the measurement of long tubes is carried out using a part holder which consists of fixed supports. For such a case, Mounaud [19] applied an upward force to each section in order to cancel the effect of gravity. Radvar-Esfahlan [5, 6] did the same using a finite element calculation.

### 1.3 The scientific issue

The main problem consists in identifying a local geometric defect (e.g. a hollow or a bump) in a globally deformed part and in proposing a functional tolerancing methodology according to ISO standards.

First, we will introduce the approach through the example of a flat part which is identified using a cloud of points obtained with a Coordinate Measuring Machine (CMM). Then, we will extend the method to the case of a complex surface, such as a blade, which is measured using a large cloud of points.

## 2. Identification methodology for the two types of defects

### 2.1 Digital straightening

#### 2.1.1 Notations

The following notations will be used throughout the paper:

$P_i$	a point on the nominal (CAD) surface
$M_i$	a measured point
$E_i$	the initial deviation between the measured point $M_i$ and the point on the nominal surface

$\mathbf{z}$	vector of the beam's axis
$\mathbf{dP}_i(dx_i, dy_i, dz_i)$	vector displacement of point $P_i$ dues to digital straightening
$\mathbf{n}_i(nx_i, ny_i, nz_i)$	vector normal to the nominal surface at $P_i$
$e_i$	the residual deviation after straightening: $e_i = E_i - \mathbf{dP}_i \cdot \mathbf{n}_i$

#### 2.1.2 Part identification

Initially, the part being studied was deliberately distorted by tightening it in a vise and applying a torque using a wrench.

Then, the distorted part was measured using a CMM. A coordinate system was defined based on 14 points in the built-in zone (the green zone on the left), and 154 points were measured in the distorted zone (the red zone on the right of Fig. 2).

#### 2.1.3 Definition of the distorted model

The global form defects were identified using a mathematical model to represent the global deformations of the part.

Considering the distortion applied to the test part, the model (Fig. 3) consists of a plane zone on the left and, on the right beyond line D, the superposition of a parabolic model representing bending and a helicoid representing torsion.

Thus, the deformed shape is characterized by the deflection  $f$  and the angle  $\alpha$  at the end of the part. The designer can choose the equations which express the deflection and the rotation.

For example, the displacement in  $y$  direction due to bending in the  $(O, x, y)$  plane on point  $P_i(x_i, y_i, z_i)$  is:

$$dy_i = f \cdot \frac{z_i^2}{L^2}$$

The angular deflection of section  $z_i$  is:

$$\alpha_i = a \cdot \frac{z_i}{L}$$

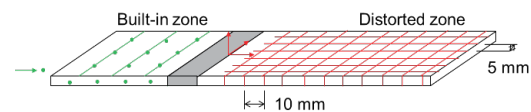


Fig. 2. The measurement of the part

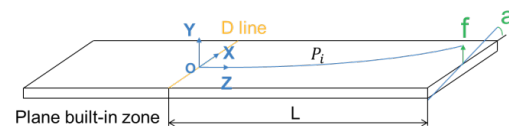


Fig. 3. The deformation model

The displacement in  $y$  direction of a point  $P_i(x_i, y_i, z_i)$  due to torsion is:

$$dy_i = a \cdot \frac{x_i \cdot z_i}{L}$$

The general expression of the deformed shape is:

$$dy_i = f \cdot \frac{z_i^2}{L^2} + a \cdot \frac{x_i \cdot z_i}{L}$$

Under the small displacement torsor assumption [7], the displacement  $dy_i$  is a linear function of parameters  $f$  and  $a$ .

Thus, the objective is to find the parameters  $f$  and  $a$  which best represent the part.

#### 2.1.4 The association principle

We chose the least-squares method to carry out the association between the actual part and the model.

The case of Fig. 2 was implemented as an Excel worksheet using the deformation model defined in 2.1.3. The measured point coordinates were used to calculate the straightened coordinates:

$$y_{\text{residual}} = y_{\text{measured}} - f \cdot \frac{(z_{\text{measured}})^2}{L^2} - a \cdot \frac{(x_{\text{measured}}) \cdot (z_{\text{measured}})}{L}$$

The objective of the least-squares method is to minimize the sum of the squared residual deviations with respect to the nominal plane  $(0, x, z)$ . In order to do that, we introduced a cell containing the sum of the squared  $y_{\text{residual}}$  into the Excel file, then minimized that cell by varying the parameters  $a$  and  $f$  thanks to the Excel solver:

$$\text{Goal} = \sum (y_{\text{residual}})^2$$

#### 2.2 Results of the digital straightening operation

The results are shown in Fig. 4.

Figure 4a shows that the part can be viewed as a twisted beam with maximum deviation  $E_{i \max} = -0.616$  mm.

Fig. 4b was obtained after digital straightening with an angle  $a = -0.0192$  rad  $\approx -1.1^\circ$  and a deflection  $f = -0.037$  mm. The residual deviations after digital straightening correspond to local defects. In that configuration, the maximum deviation was  $e_{i \max} = 0.192$  mm.

The fact that the residual deviation  $e_{i \max}$  is smaller than  $E_{i \max}$  proves that the proposed model represents the part's actual shape quite well.

The deflection thus applied enables one to identify the bending defect. The negative value of  $f$  along the  $y$ -axis

shows that in the actual shape one end points downwards (Fig. 4a). The negative angle represents a negative twisting about the  $z$ -axis.

#### 2.3 Evolution of the sections

The residual deviations at each point after digital straightening characterize the part. The principle of the method consists in associating each section with a nominal profile and using the least-squares method to minimize the deviation between the nominal profile and the measured points (Fig. 5). Each section is characterized by two parameters, a translation  $w$  of the center of the section and a rotation  $\delta$ .

The evolution of the two parameters  $w$  and  $\delta$  of several sections of the part after digital straightening (Fig. 6) gives a good indication of the defects along the  $z$ -axis of the part. In that particular case, the evolution is smooth, but this figure could also have shown a wave or a jump, which could have been unacceptable.

Today, there is no specification enabling one to tolerance this continuity of the evolution of sections. A general

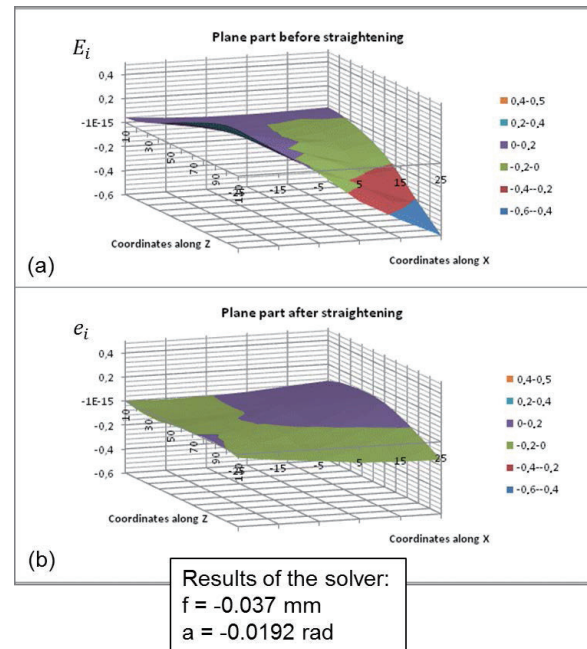


Fig. 4. Deviations  $E_i$  of the plane part (a) and deviations  $e_i$  after digital straightening (b)

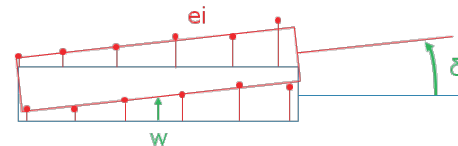


Fig. 5. Deviations of a section after straightening

definition of the “straightness of the part’s axis” could be introduced at the center of each section, which would require the construction of the axis of a part of any shape.

## 2.4 Tolerancing of the part

The ISO 10579 standard [2] enables one to define a protocol for straightening a part. This straightening is usually achieved by applying loads, e.g. by holding the part with clamps.

The originality of our approach is that straightening is not performed physically, but digitally. Therefore, tolerancing must be expressed by an equation which characterizes this digital straightening (Fig. 7). Consequently, this makes it possible to specify the shape of a side, of a section or of the entire part.

The tolerances marked “F” (for “free”) must be satisfied in the free state, *i.e.* without straightening, with deviations  $E_i$ . The unmarked tolerances must be satisfied in the stressed state after digital straightening, *i.e.* with the deviations  $e_i$  (Fig. 8).

## 2.5 Other examples of distorted models

Regardless of the part’s configuration, its global defects

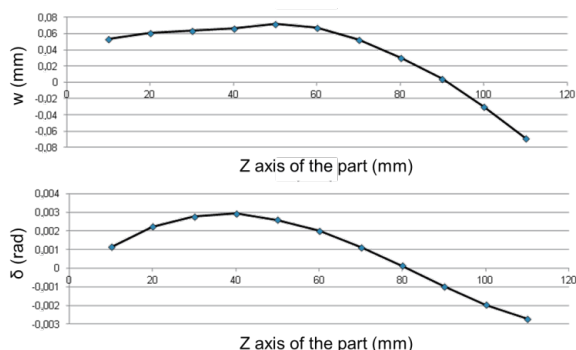


Fig. 6. Evolution of the position and orientation parameters of the part’s sections

must be defined using a parametric model.

For a cylindrical part, it is easy to define a model using 4 parameters:

- the cone angle
- the base radius
- the ovality
- the radial deflection at the center of the generatrix.

For large beam-like parts with constant cross sections, many bending models can be imagined depending on the loading cases and boundary conditions applied to the beam. This work proposes two deformation modes for this type of part:

**Mode 1:** (Fig. 9) Built-in condition at A and deflection at B with a readjustment of the beam’s direction and the base coordinate system through two parameters,  $\text{decY}_{(\text{bottom})}$  and  $\text{decY}_{(\text{top})}$ . By similarity with the bending of a beam with constant cross section, the deformed shape is a polynomial of degree 3.

	0.04	After digital straightening
	0.2 (F)	Free state

Fig. 8. Specifications relative to the free state and after digital straightening

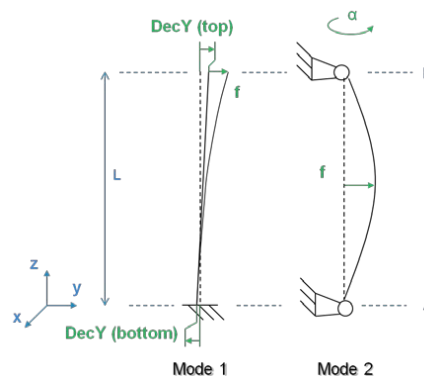


Fig. 9. Examples of deformation modes

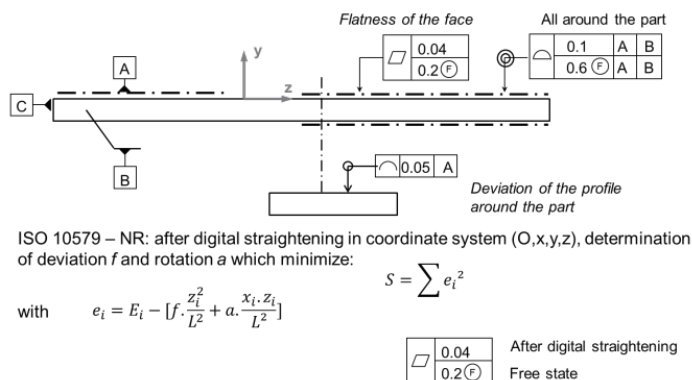


Fig. 7. Tolerancing of the part



**Mode 2:** (Fig. 9) Pinned connections (i.e. no translations) at ends A and B, and a deflection  $f$  at the center of the beam. Twisting of the part around the  $z$ -axis with angles  $a$  at B and 0 at A (Fig. 9 and 10).

For the second mode, a twist angle is applied at B. The resulting shape is a helicoid (Fig. 10). If the angle is too large, it is necessary to determine the displacements of some points along the  $x$  and  $y$  axes because the small displacement assumption [7] is not satisfied.

For each model, the equations giving the displacement at each point must be defined using the following parameters:

- $a$  the rotation angle
- $f_x, f_y$  the deflections in  $x$  and  $y$  direction (Fig. 9)

**Mode 1:**

The displacement of point  $P_i$  is decomposed in  $x$  and  $y$  directions:

$$dx_i = \frac{DecX_{(bottom)} \cdot (L - z_i) + DecX_{(top)} \cdot z_i}{L} + f_x \cdot \frac{-z_i^3 + 3L \cdot z_i^2}{2L^3}$$

$$dy_i = \frac{DecY_{(bottom)} \cdot (L - z_i) + DecY_{(top)} \cdot z_i}{L} + f_y \cdot \frac{-z_i^3 + 3L \cdot z_i^2}{2L^3}$$

**Mode 2:**

$0 < z < L/2$ :

$$dx_i = f_x \cdot \frac{-4z_i^3 + 3L^2 \cdot z_i}{L^3} + a \cdot z_i \cdot \frac{y_c - y_i}{L}$$

$$dy_i = f_y \cdot \frac{-4z_i^3 + 3L^2 \cdot z_i}{L^3} + a \cdot z_i \cdot \frac{x_i - x_c}{L}$$

$L/2 < z < L$ :

$$dx_i = f_x \cdot \frac{-4(L - z_i)^3 + 3L^2 \cdot (L - z_i)}{L^3} + a \cdot z_i \cdot \frac{y_c - y_i}{L}$$

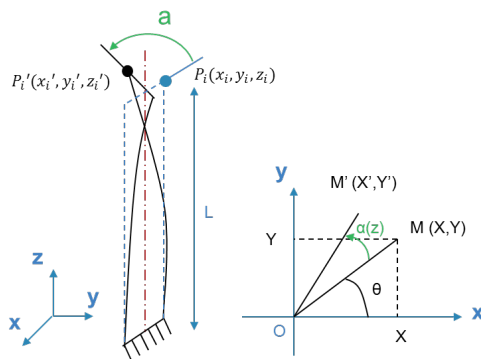


Fig. 10. A twisted model

$$dy_i = f_y \cdot \frac{-4(L - z_i)^3 + 3L^2 \cdot (L - z_i)}{L^3} + a \cdot z_i \cdot \frac{x_i - x_c}{L}$$

Other models can be created, e.g. for parts with varying sections. The finite element method can be used to calculate the deflection at each point under a nominal force or moment [5], [6]. Due to the linearity assumption, one obtains the deformed shape as a function of the force and moment.

By comparing several calculation criterions, one can select parameter values which minimize the sum of the deviation absolute values

### 3. Application to complex industrial surface

#### 3.1 Application to a turbine blade

In the context of the manufacturing of aeronautical parts, Snecma wishes to improve its understanding of the deviations measured on turbine blades (Fig.11). Indeed, the measured deviations can be due to various types of defects on different scales. For example, a 0.05 mm distortion along the trailing edge has a greater impact on performance than a 0.3 mm global defect due to twisting of the part. However, the former generates turbulences, whereas the latter only deflects the air flow.

Our approach was applied to a blade designed by Snecma using a cloud of points, spanning the entire part (about 600,000 points), obtained by means of an optical measuring tool [20].

The main objective was to quantify the deviations  $E_i$  between the actual part and the nominal geometry, then the deviations  $e_i$  between the actual part and the distorted geometry.

#### 3.2 Identification of the global form defects

Two studies were carried out using the deformation

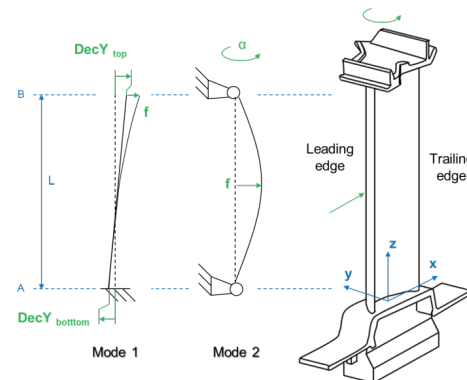


Fig. 11. The blade model

modes defined previously:

- clamping of the blade at its base in the turbine wheel, with no twisting (Fig. 11, Mode 1)
- a deflection in the central area of the blade with a twist (Fig. 11, Mode 2)

### 3.3 Calculation of the amplitudes of the global defects

#### 3.3.1 Initial registration

The measurements were performed by Snecma using an optical system developed by GOM [20], which consists in a stereovision device projecting an array of blue fringes (to avoid interaction with the natural light [4]).

The points were measured in a measurement coordinate system. The first fitting of the point cloud with the CAD model was achieved by considering several surfaces and matching 6 target points with the corresponding CAD surfaces (Fig. 12). These surfaces were not machined and provided a constant coordinate system throughout the manufacturing process. This is the raw reference frame.

The time required to perform these operations (acquisition

of the point cloud and registration) was about 10 minutes for an accurate view of the whole part with triangulation, but the initial setting is time-consuming (about 4 hours), so profitability is very dependent on the number of parts measured.

#### 3.3.2 Point extraction for straightening

The objective is to determine the straightening parameters, particularly deflection and twisting, to be applied to the point cloud in order to minimize the sum of the squared deviations. The Excel solver was used so the operation would remain as generic as possible.

In order to avoid numerical problems and excessive computation time because of too many points, the calculation was performed on only a few sections (Fig. 13).

The least-squares calculation requires that the real point  $M_i$  coordinates and the normal  $n_i$  components of the surface are known.

The construction of the sample is illustrated in Fig. 14. The optical measurements lead to a cloud of real points and a triangular mesh connecting these points. The expected

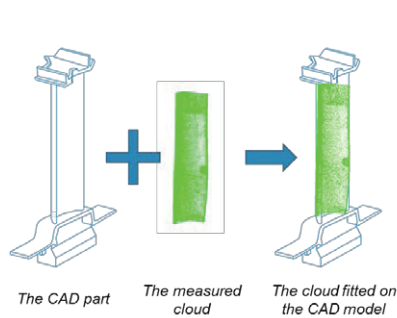


Fig. 12. The fitting of the cloud of points

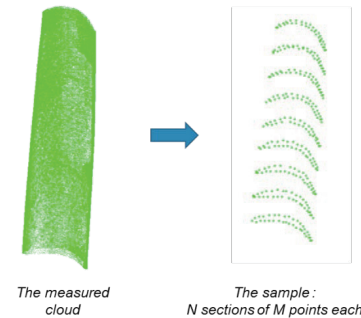


Fig. 13. The measured cloud and the sample extracted

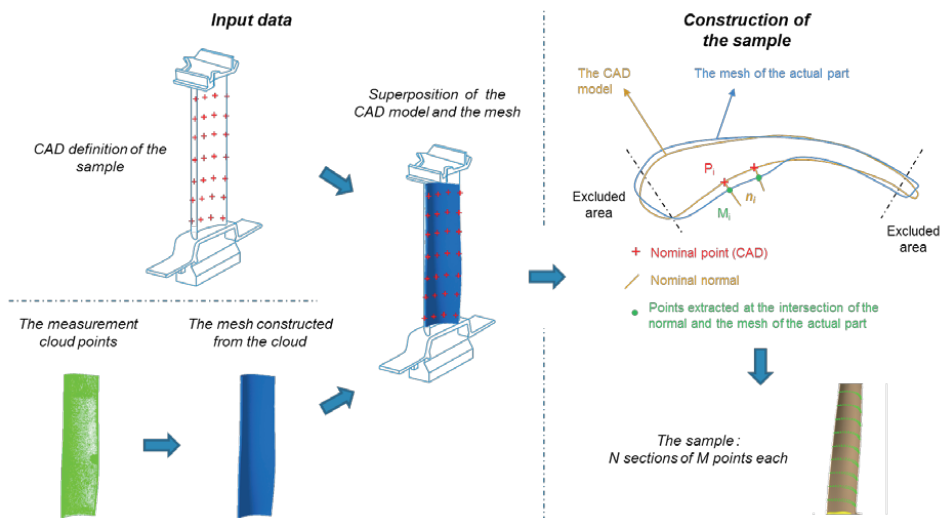


Fig. 14. Construction of the sample for the calculation of the straightening parameters

sections are generated in the CAD system by extracting a small number of nominal points  $P_i$  along the section line (38 points per section in this particular experiment). At each point  $P_i$  of a nominal section, the deviation  $E_i$  between the mesh and the CAD model is defined along the normal  $\mathbf{n}_i$ . The lines  $(P_i, \mathbf{n}_i)$  and the mesh intersect at points  $M_i$  considered as real points:

$$E_i = {}^tP_i M_i \cdot \mathbf{n}_i$$

The points along the trailing edge are excluded from the calculation because the local radius is too small and the normal vectors are not constant with regard to deviation dues to twist.

Thus, each section is characterized by a series of nominal points  $P_i$  from the CAD model, the normal  $\mathbf{n}_i$  at each point and the deviation  $E_i$  with respect to the actual surface materialized by the mesh of the measured points.

This extraction was automated through a quick development in the CATIA CAD software. As written before and in order to avoid numerical problems due to the curvature, the sample distribution was created without taking into account the leading and trailing edges.

### 3.3.3 Calculation of the distorted model's parameters using the Excel solver

After the straightening operation, the deviations become  $e_i$ :

$$e_i = E_i - {}^t dP_i \cdot \mathbf{n}_i$$

The calculation of the straightening / torsion parameters for the sample defined previously answers to the following problem:

**Mode 1:** Find  $(decX_{(bottom)}; decX_{(top)}; decY_{(bottom)}; decY_{(top)}; fx; fy)$

**Mode 2:** Find  $(\alpha; fx; fy)$  which minimise  $\sum e_i^2$ ,

with  $e_i = E_i - {}^t dP_i \cdot \mathbf{n}_i$

At each point  $P_i$ , the deformation models lead to  $dx_i$  and  $dy_i$  according to chosen mode.

Then, the Excel solver changes the values of the parameters in order to minimize the sum of the squared deviations. The computation time is only a few seconds, depending on the size of the sample.

Another calculation could minimize the sum of the shape defects in the 9 sections by minimizing:

$$D = 2 \sum_{j=1}^9 \text{Max}(|e_i|)$$

One advantage of that method would be that the calculation would be unaffected by the density of the point cloud.

### 3.4 Digital straightening of the actual part

With the values obtained, a displacement field was applied to the whole set of the measured points.

Then, the new cloud of points obtained after digital straightening was imported into CATIA for comparison with the nominal model. Finally, the residual deviations (local defects) were obtained through a deviation analysis and plotted as a color map (Fig. 15).

The values obtained (hidden for confidentiality) show the global shape defects of the blade (deflection and twisting).

The color map of the residual deviations characterizes the local defects of the surface. In our example, the main defects, before digital straightening, are a lack of material on the suction side of the leading edge and an excess of material on the pressure side. After digital straightening we note that some deviations were due to global defects.

### 3.5 Blade tolerancing

As explained in Section 2.4 in the case of a simple example, this geometric analysis method can be specified with tools of the ISO 10579 standard [2], leading to the definition of a stressed state.

Figure 16 shows the blade case with deformation Mode 1. The coordinate system is defined directly on the CAD model created from the measurement cloud.

As mentioned before, the specifications can be controlled at two different states (stressed or free), depending on the presence of modifier  $F$ . So there are two dedicate check procedures for both case.

The first one, with  $F$  modifier, consists to verify if the measurement cloud is included in the tolerance zone, defined by the ISO specification, immediately after the measurement clouds registration on the datum reference frame of the CAD model. In that case no digital straightening is realized, this is the “free” state.

In the second case, without  $F$  modifier, the measurement cloud is fitted on the CAD model next digitally straighten in a “stressed” state defined by defect modes, then straighten points cloud is compared to the tolerance zone.

The last two figures correspond to the industrial requirement to analyze the defects and validate the conformity of a blade.

## 4. Conclusion

The digital straightening method presented in this work can be applied to slender parts with constant or variable sections, or even to thin parts such as sheet metal or



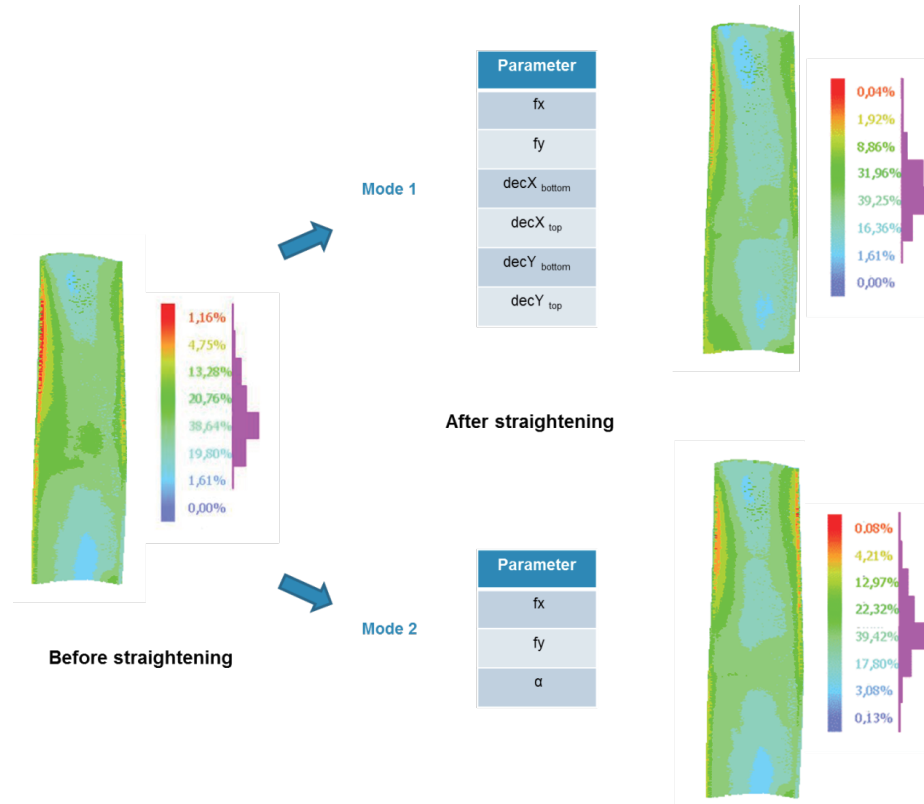


Fig. 15. Comparison before / after digital straightening depending on the mode selected

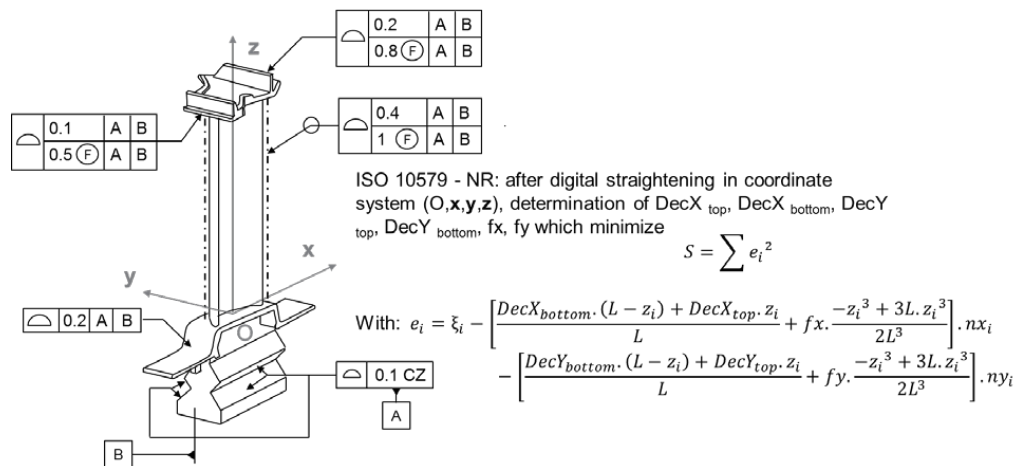


Fig. 16. Blade tolerancing by digital straightening with ISO 10579

crankcases, once the deformation model has been chosen.

The ISO tolerancing proposed is based on a dual specification in the free state and in the straightened state through a digital process, leading to the deformation equation and the objective function to be minimized.

In the case of the simple part discussed in section 2, the measurements were carried out by means of a measuring

machine. For the blade, the measurement of a large point cloud was performed using an optical device.

In both cases, the model's parameters characterized the general shape of the part. The residual deviations after straightening led to the representation of the local defects.

Several types of straightening models can be tested in order to identify the global shape deviations and the smaller

residual deviations of the part. In addition, the smoothness of the variation in the directions of the part's sections can be described.

The residual defects can be easily visualized as color maps. The corresponding computation time is small (only a few seconds), but the time required for the measurements remains too long (4 hours setup time + 10 minutes per part for the measurements and triangulation). Today, this method can be used only to qualify a manufacturing process or to perform a sample measurement during production.

New portable optical measurement systems should make it possible to measure parts directly in the workshop and to check raw parts and machined workpieces in only a few seconds.

However, additional effort is required in order to be able to adjust the density of the point clouds for determining the straightening parameters, especially at the leading and trailing edges, using the least-squares criterion and comparing the results with those of the minimization criterion of the sum of the sectional shape defects.

The demonstrator which has been achieved meets the needs of Snecma Company. The company decided to integrate this application into the CATIA environment to use it in the central metrology services, especially to validate the production process of raw or finished blades.

## Acknowledgement

The authors wish to thank Snecma for welcoming them in an internship at Gennevilliers and Villaroche in 2012 and for providing the measurements used in their study. This work was carried out under the Quick GPS project, labeled System@tic and Astech, funded by the "Region Ile de France".

## References

- [1] ISO 1101 standard: 2013, Geometrical product specifications (GPS) – Geometrical tolerancing – Tolerances of form, orientation, location and run-out.
- [2] ISO 10579 standard: 2010, Geometrical product specifications (GPS) – Dimensioning and tolerancing – Non-rigid-parts.
- [3] Li, Y. and Gu, P., "Free-form surface inspection techniques state of the art review", *Computer-Aided Design*, Vol. 36, 2004, pp. 1395-1417.
- [4] Savio, E., De Chiffre, L. and Schmitt, R., "Metrology

of freedom shaped parts", *CIRP Manufacturing Technology*, Elsevier, Vol. 56, 2007, pp. 810-835.

[5] Radvar-Esfahlan, H. and Tahan, S-A., "Nonrigid geometric metrology using generalized numerical inspection fixtures", *Precision Engineering*, Vol. 36, 2011, pp. 1-9.

[6] Radvar-Esfahlan, H. and Tahan, S-A., "Robust generalized numerical inspection fixture for the metrology of compliant mechanical parts", *The International Journal of Advanced Manufacturing Technology*, Vol. 70, 2013, pp. 1101-1112.

[7] Bourdet, P., Mathieu, L., Lartigue, C. and Ballu, A., "The concept of the small displacement torsor in metrology", *Advanced mathematical tools in metrology II*, Series on advances in mathematics for applied sciences, Vol. 40, 1996, pp. 110-122.

[8] Zhu, L., Barhak, J., Srivatsan, V. and Katz, R., "Efficient registration for precision inspection of free-form surfaces", *The International Journal of Advanced Manufacturing Technology*, Vol. 32, 2007, pp. 505-515.

[9] Samper, S. and Formosa, F., "Form Defects Tolerancing by natural Modes Analysis", *Journal of computing and information science in engineering*, Vol. 7, 2007, pp. 44-51.

[10] Adragna, P. A., Samper, S. and Pillet, M., "Analysis of shape deviations of measured geometries with a modal basis", *Journal of Machine Engineering : Manufacturing Accuracy Increasing Problems, Optimization*, Vol. 6, No. 1, 2006, pp. 95-102.

[11] Formosa, F., Samper, S. and Perpoli, I., "Modal expression of form defects", *Models for computer aided tolerancing in design and manufacturing*, Springer series, 2007, pp. 13-22.

[12] Favreliere, H., Samper, S., Adragna, P-A. and Giordano, M., "3D statistical analysis and representation of form error by a modal approach", *10th CIRP International Seminar on Computer-Aided Tolerancing*, 2007.

[13] Capello, E. and Semeraro, Q., "Harmonic fitting approach for plane geometry measurements", *The international journal of advanced manufacturing technology*, Vol. 16, 2000, pp. 250-258.

[14] Huang, W. and Ceglarek, D., "Mode-based decomposition of part form error by discrete-cosine-transform with implementation to assembly stamping system with compliant parts", *Annals of the CIRP*, Vol. 51, No. 1, 2002, pp. 21-26.

[15] Summerhays, K. D., Henke, R. P., Baldwin, J. M., Cassous, R. M. and Brown, C. W., "Optimizing discrete point sample patterns and measurement date analysis on internal cylindrical surfaces with systematic form deviations", *Journal of the International Society for Precision Engineering*, Vol. 26, 1, 2002, pp. 105-121.

[16] Henke, R. P., Summerhays, K. D., Baldwin, J. M., Cassous, R. M. and Brown, C. W., "Methods for evaluation of systematic geometric deviations in machined parts and their relationships to process variables", *Precision engineering*, Vol. 23, 1999, pp. 273-292.

[17] Cho, N. and Tu, J., "Roundness modeling of machined parts for tolerance analysis", *Journal of the International Societies for Precision Engineering and Nanotechnology*, Vol. 25, 2001, pp. 35-47.

[18] Damir, M. N. H., "Approximate harmonic models for roundness profiles", *WEAR*, Vol. 57, 1979, pp. 217-225.

[19] Mounaud, M., Thiébaud, F., Bourdet, P., Falgarone, H. and Chevassus, N., "Integrating the flexibility of components in the assembly of aeronautics hydraulic systems", *10<sup>th</sup> CIRP International Seminar on Computer Aided Tolerancing*, Erlangen, Germany, 2007.

[20] <http://www.gom.com/metrology-systems/3d-scanner.html>